

Doping-dependent anisotropic superconducting gap in $\text{Na}_{1-\delta}(\text{Fe}_{1-x}\text{Co}_x)\text{As}$ from London penetration depth

K. Cho,^{1,2} M. A. Tanatar,^{1,2} N. Spyridis,^{1,2} H. Kim,^{1,2} Y. Song,³ Pengcheng Dai,³ C. L. Zhang,³ and R. Prozorov^{1,2,*}

¹The Ames Laboratory, Ames, Iowa 50011, USA

²Department of Physics and Astronomy, Iowa State University, Ames, Iowa 50011, USA

³Department of Physics and Astronomy, The University of Tennessee, Knoxville, Tennessee 37996, USA

(Received 13 January 2012; revised manuscript received 5 July 2012; published 30 July 2012)

The London penetration depth was measured in single crystals of self-doped $\text{Na}_{1-\delta}\text{FeAs}$ (from under doping to optimal doping, T_c from 14 to 27 K) and electron-doped $\text{Na}(\text{Fe}_{1-x}\text{Co}_x)\text{As}$ with x ranging from undoped, $x = 0$, to overdoped, $x = 0.1$. In all samples, the low-temperature variation of the penetration depth exhibits a power-law dependence, $\Delta\lambda(T) = AT^n$, with the exponent that varies in a dome-like fashion from $n \sim 1.1$ in the underdoped, reaching a maximum of $n \sim 1.9$ in the optimally doped, and decreasing again to $n \sim 1.3$ on the overdoped side. While the anisotropy of the gap structure follows a universal dome-like evolution, the exponent at optimal doping, $n \sim 1.9$, is lower than in other charge-doped Fe-based superconductors (FeSCs). The full-temperature range superfluid density, $\rho_s(T) = [\lambda(0)/\lambda(T)]^2$, at optimal doping is also distinctly different from other charge-doped FeSCs but is similar to isovalently substituted $\text{BaFe}_2(\text{As}_{1-x}\text{P}_x)_2$, believed to be a nodal pnictide at optimal doping. These results suggest that the superconducting gap in $\text{Na}(\text{Fe}_{1-x}\text{Co}_x)\text{As}$ is highly anisotropic even at optimal doping.

DOI: 10.1103/PhysRevB.86.020508

PACS number(s): 74.70.Xa, 74.20.Rp, 74.62.Dh

Fe-based superconductors (FeSCs) represent a rich variety of materials.^{1–5} Despite this chemical diversity, a generic trend is that a superconducting “dome” in the temperature versus doping phase diagram forms in the vicinity or coexists with the long range magnetic order. Instability of the electronic system caused by the proximity of magnetism and superconductivity is considered as a key to understanding the pairing mechanism in the FeSCs.¹ Contrary to cuprate high-temperature superconductors, which show a robust nodal d -wave superconducting gap for all doping types and levels, the gap structure of FeSCs is strongly doping dependent, varying from an isotropic to nodal gap structure.^{3–9} An important question at this moment is whether there is any universality in the doping dependence of the gaps among different FeSC materials.

The universal trend was suggested in studies of the 122 family. In particular, the gap structure of both electron-doped $\text{Ba}(\text{Fe}_{1-x}\text{T}_x)_2\text{As}_2$ (“BaT122,” T = transition metal)^{6–12} and hole-doped $(\text{Ba}_{1-x}\text{K}_x)\text{Fe}_2\text{As}_2$ (“BaK122”)^{13–16} are nodeless and isotropic at optimal doping and become highly anisotropic (perhaps nodal) at the dome edges. The isovalent-doped $\text{LiFe}(\text{As},\text{P})$ (Refs. 17 and 18) and layered $\text{Ca}_{10}(\text{Pt}_3\text{As}_8)[(\text{Fe}_{1-x}\text{Pt}_x)_2\text{As}_2]_5$ (“Ca10-3-8”) compounds¹⁹ obey this trend as well. The only exception to this universal trend is found in isovalent-doped materials such as $\text{BaFe}_2(\text{As}_{1-x}\text{P}_x)_2$ (“BaP122”) (Refs. 20 and 21) and $\text{Ba}(\text{Fe}_{1-x}\text{Ru}_x)_2\text{As}_2$,²² where nodal behavior was concluded even at optimal doping. It was suggested by Kuroki *et al.* that nodal versus nodeless behavior is controlled by the pnictogen height at least in a 1111 ($R\text{FeAsO}$, where R = rare earth metal) family,²³ and Hashimoto *et al.* extended this suggestion to 111 ($A\text{FeAs}$, where A = Alkali metal) and 122 families.¹⁸ It is also believed that the same parameter controls the transition temperature T_c .^{24,25} Other factors that might control the nodal versus nodeless gap are the doping-dependent electronic band structure and competition between intraband and interband

interactions, taking into account the different orbital contents in each band.^{3,4,26} Therefore, it is important to study other Fe-based systems to test these ideas and determine possible universal trends, if they exist.

Stoichiometric NaFeAs is isostructural with LiFeAs ($T_c \sim 18$ K) and it exhibits bulk antiferromagnetic order and filamentary superconductivity.²⁷ Application of 3 GPa pressure raises T_c to 31 K, indicating its effective underdoped nature²⁸ that is distinct from the slightly overdoped nature of stoichiometric LiFeAs .²⁹ Supporting this underdoped nature of parent NaFeAs , a coexistence of magnetism and superconductivity was found in NMR, neutron scattering, electronic transport, and muon spin rotation (μSR) measurements.^{30–33} The coexistence region extends to optimally doped $\text{NaFe}_{1-x}\text{Co}_x\text{As}$ with electron Co-substituted Fe.³¹ The angle-resolved photoemission spectroscopy (ARPES) study in near optimally doped $\text{NaFe}_{0.95}\text{Co}_{0.05}\text{As}$ revealed quasinested Fermi surfaces connected by a $Q = (\pi, \pi)$ wave vector, suggesting an important role of magnetic instability in superconductivity,³⁴ similar to the 122 family. This is in stark contrast to the absence of nesting in LiFeAs ,³⁵ despite recent reports from inelastic neutron scattering, indicating incommensurate magnetic correlation in LiFeAs .³⁶ The gaps obtained in the ARPES study in $\text{NaFe}_{0.95}\text{Co}_{0.05}\text{As}$ are isotropic.³⁴ However, they persist well above T_c and thus are unlikely related to superconductivity. Scanning tunneling spectroscopy revealed V-shaped curves,³⁷ which may be consistent with both nodal and nodeless gaps. Specific heat measurements revealed a jump at T_c , but did not extend to low enough temperature to reveal characteristic nodal versus nodeless behavior.³⁸ Considering the ambiguity of the phonon contribution subtraction and multigap nature of superconductivity in the FeSCs, in the current stage the specific heat results cannot rule out the existence of (at least one) highly anisotropic gap. Therefore the important question on the anisotropy of superconducting gaps in $\text{NaFe}_{1-x}\text{Co}_x\text{As}$ remains open.

In this Rapid Communication, we study the doping evolution of the superconducting gap structure in NaFeAs single crystals using a high resolution tunnel-diode resonator (TDR) technique. The doping level was controlled with either self-doping in $\text{Na}_{1-\delta}\text{FeAs}$ caused by environmental oxidative deintercalation (underdoped to an optimally doped range) or Co doping in $\text{Na}(\text{Fe}_{1-x}\text{Co}_x)\text{As}$ (spanning the whole superconducting dome). We found that, similar to most FeSCs, the variation of the London penetration depth is best described by a power-law function, $\Delta\lambda = AT^n$, with the exponent n and prefactor A varying systematically with doping in a dome-like fashion. The values of n in the underdoped ($n \sim 1.1$) and heavily overdoped ($n \sim 1.3$) compositions strongly suggest a superconducting gap with line nodes. Even at optimal doping the exponent $n \sim 1.9$ is notably lower than in the other charge-doped FeSCs.⁵ The superfluid density $\rho_s(T)$ at optimal doping is also incompatible with an isotropic full gap. Instead, $\rho_s(T)$ at $x = 0.05$ is remarkably similar to that of optimally isovalent-doped $\text{BaFe}_2(\text{As}_{1-x}\text{P}_x)_2$, a known nodal pnictide superconductor even at optimal doping.²⁰ Our observations suggest that, despite the universal tendency for highest anisotropy at the dome edges in $\text{LiFe}(\text{As,P})$,^{17,18} BaCo122 ,⁹ BaK122 ,¹³ and a layered Ca10-3-8 system,¹⁹ the gap structure at the dome center can be highly anisotropic even in the charge-doped systems.

Single crystals of $\text{Na}(\text{Fe}_{1-x}\text{Co}_x)\text{As}$ with $x = 0, 0.02, 0.025, 0.05, 0.08,$ and 0.10 were synthesized by sealing in the mixture of Na, Fe, As, and Co together in Ta tubes and heating at 950°C , followed by 5°C/h cooling down to 900°C .³⁹ We determined x as used in the load to crystal growth. The samples were stored and transported in sealed containers filled with an inert gas. The sample preparation for TDR measurements was done quickly in air within about 5 min to minimize uncontrolled environmental exposure which can induce an increase of T_c .^{40,41} The process of bulk “self-doping” can be well controlled using a reaction with Apiezon N grease, and can be facilitated by an ultrasonic treatment stimulating deintercalation of Na^+ ions. The duration of the sonication treatment was used to control T_c of the sample (see Ref. 41 for details). The low-temperature variation of the in-plane London penetration depth $\Delta\lambda(T)$ was measured using the TDR technique described elsewhere.^{5,42,43}

Figure 1 shows the low-temperature variation of $\Delta\lambda(T)$ in two samples A and B of $\text{Na}_{1-\delta}\text{FeAs}$ crystals, which shows a clear evolution from almost T -linear (pristine) to almost quadratic (1-h ultrasonic treatment) behavior. Measurements were done immediately after opening the ampoule (pristine state) and repeated after a 1-h ultrasonic treatment, which increased T_c to 22 K (see the inset). Successive treatments increased T_c to a maximum value of ~ 27 K (after 2- and 3-h treatments), but longer treatments lead to sample degradation.

Figure 2 shows the low-temperature variation of $\Delta\lambda(T)$ in $\text{Na}(\text{Fe}_{1-x}\text{Co}_x)\text{As}$ for $x = 0.02, 0.025, 0.05, 0.08,$ and 0.10 . Judging by $T_c(x)$ in the inset, the samples cover the superconducting dome from a lightly underdoped to a heavily overdoped regime. For a quantitative analysis of low-temperature behavior, a fit to power-law function, $\Delta\lambda(T) = AT^n$, was performed over a temperature interval from the base temperature up to several upper limits, varying from $T_c/10$ to

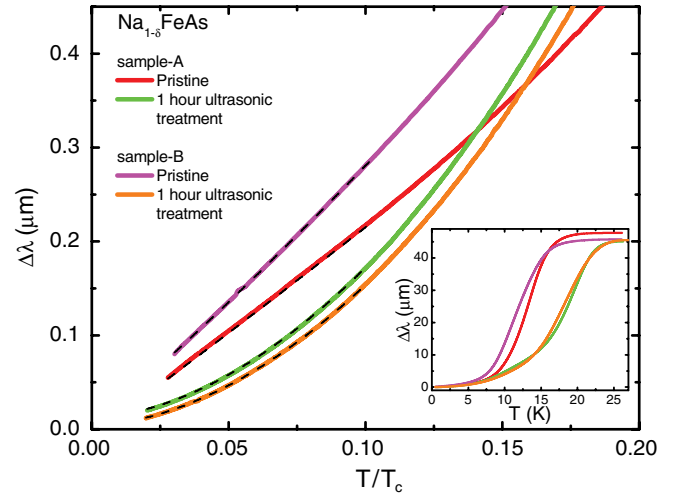


FIG. 1. (Color online) Low-temperature part of $\Delta\lambda(T/T_c)$ in two $\text{Na}_{1-\delta}\text{FeAs}$ samples (A and B) in pristine and ultrasonic treated (1-h) states. Dashed lines are representative power-law fits up to $T/T_c = 0.1$ for a quantitative analysis. The inset shows a full-temperature range variation of $\Delta\lambda(T)$ for the same samples.

$T_c/5$. The representative fits for $T_c/5$ limit are shown as dashed lines.

Figure 3 presents a summary of our results for NaFeAs system. A doping dependence of T_c [Fig. 3(a)] in $\text{Na}(\text{Fe}_{1-x}\text{Co}_x)\text{As}$ is shown against actual x (bottom axis). The data for $\text{Na}_{1-\delta}\text{FeAs}$ are plotted against the sonication time (top axis) after scaling that the maximum T_c is matched with that from the Co-doped case (i.e., 2.5-h sonication treatment equivalent to $x = 0.025$). The parameters of the power-law fit, $\Delta\lambda(T) = AT^n$, are summarized in Figs. 3(b) and 3(c). For each data set, fitting was performed for several temperature ranges to examine the robustness of the fitting parameters. In $\text{Na}_{1-\delta}\text{FeAs}$, the exponent n is about 1.1 in the most underdoped

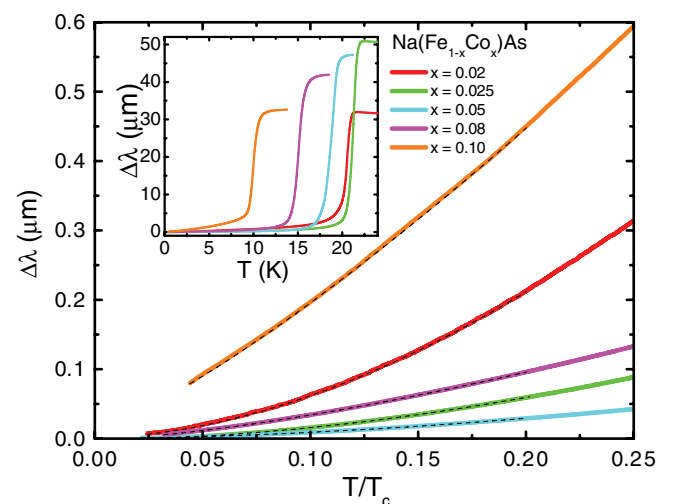


FIG. 2. (Color online) (a) Low-temperature part of $\Delta\lambda(T/T_c)$ in $\text{Na}(\text{Fe}_{1-x}\text{Co}_x)\text{As}$ for $x = 0.02, 0.025, 0.05, 0.08,$ and 0.10 . Dashed lines are representative power-law fits up to $T/T_c = 0.2$ for a quantitative analysis. Fitting results are summarized in Fig. 3. The inset shows a full-temperature range variation of $\Delta\lambda(T)$ for the same samples.

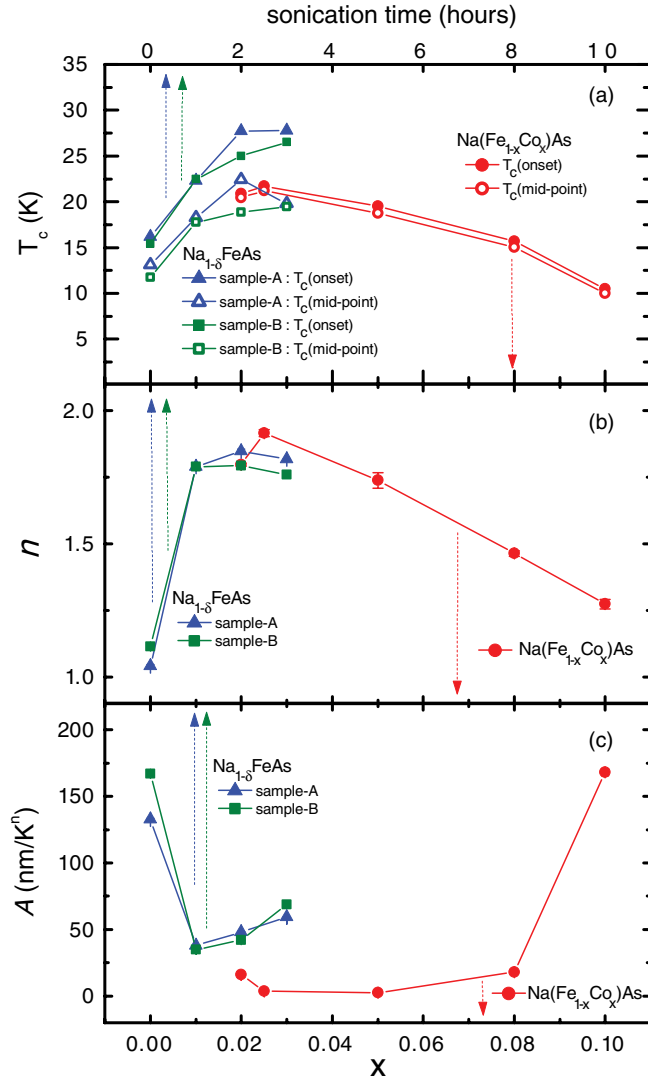


FIG. 3. (Color online) Phase diagram of NaFeAs system. (a) Superconducting “dome” $T_c(x)$, (b) power-law exponent $n(x)$, and (c) prefactor $A(x)$. The results of self-doping study were placed against sonication time (top axis) and scaled by their T_c (see text). Circles show the data for Co-doped samples. Other symbols show the data for self-doped samples.

composition (pristine samples) and increases to 1.8 after 3-h sonication when the highest $T_c \approx 27$ K is reached. Similarly, a larger exponent, $n \sim 1.9$, was obtained in $\text{Na}(\text{Fe}_{1-x}\text{Co}_x)\text{As}$ for $x = 0.025$ (optimal doping) and it monotonically decreased to $n \sim 1.3$ for overdoped $x = 0.10$. In general, the results for both $\text{Na}_{1-\delta}\text{FeAs}$ and $\text{Na}(\text{Fe}_{1-x}\text{Co}_x)\text{As}$ follow a universal trend that the gap anisotropies are highest at the dome edges and smallest at the dome center. The values at the dome edges are notably below the lowest possible value ($n \sim 1.7$) expected from the s_{\pm} scenario with strong pair-breaking scattering,⁵ suggesting the formation of nodes. In addition, the low value of the exponent $n \sim 1.9$ at the dome center makes a clear distinction of $\text{Na}_{1-\delta}(\text{Fe}_{1-x}\text{Co}_x)\text{As}$ from the other chargedoped FeSCs. The exponents close to $n \sim 2$ can be explained by a strong pair-breaking effect in s_{\pm} - or d -wave pairing scenarios.

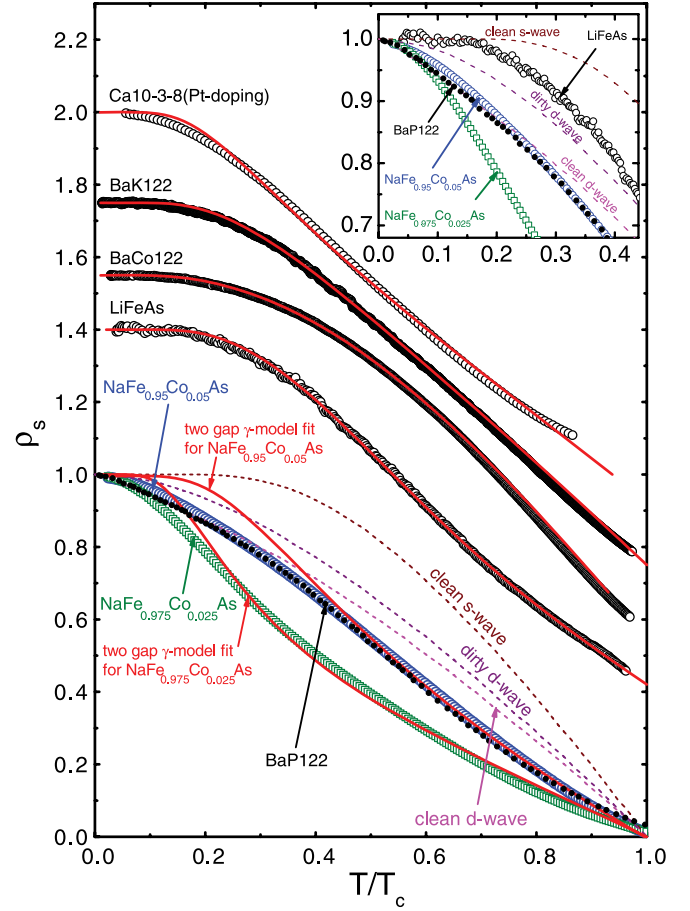


FIG. 4. (Color online) Experimental normalized superfluid densities $\rho_s(T)$ of optimally doped FeSCs. The top four curves for LiFeAs (Ref. 17), BaCo122 (Ref. 5), BaK122 (Ref. 13), and Ca10-3-8 (Ref. 19) were offset for clarity. Red solid curves show the best fits to an isotropic s -wave two-gap γ model (Ref. 44), demonstrating good agreement with the data. In clear contrast, the ρ_s for optimally doped $\text{NaFe}_{0.975}\text{Co}_{0.025}\text{As}$ (green open squares) and $\text{NaFe}_{0.95}\text{Co}_{0.05}\text{As}$ (blue open circles) cannot be fitted with this fully gapped model, especially at the lowest temperatures, zoomed in at in the inset. For comparison, we also show the data for optimally doped BaP122 ($x = 0.33$, black solid dots) (Ref. 20) as well as single d and s gaps (dashed lines) in both clean and dirty limits.

For a more complete analysis of the superconducting gap structure, especially in a multigap system, the low-temperature power-law behavior is not sufficient, as it only reflects quasiparticle excitations around the gap minima. Figure 4 shows a normalized superfluid density, $\rho_s(T) = [\lambda(0)/\lambda(T)]^2$, plotted against T/T_c for several optimally doped FeSCs. To calculate ρ_s in $\text{NaFe}_{0.975}\text{Co}_{0.025}\text{As}$ (green open squares) and $\text{NaFe}_{0.95}\text{Co}_{0.05}\text{As}$ (blue open circles), we used the values of $\lambda_0 = 410$ and 354 nm, respectively, obtained from μSR measurements.³¹ The ρ_s for other materials (offset vertically for clarity in Fig. 4) include LiFeAs,¹⁷ BaCo122,⁵ BaK122,¹³ and Ca10-3-8,¹⁹ all measured in our group. Red solid curves are the best fits to a self-consistent isotropic s -wave two-gap γ model,⁴⁴ showing good fit quality in all four cases. In stark contrast, an attempt to fit the data for $\text{NaFe}_{0.975}\text{Co}_{0.025}\text{As}$ and $\text{NaFe}_{0.95}\text{Co}_{0.05}\text{As}$ (both are near optimal doping) with the same

γ model clearly fails, especially at the low-temperature end, where the distinction between full and nodal gaps is most pronounced, as zoomed in the inset of Fig. 4. For comparison, we also show $\rho_s(T/T_c)$ expected for single-gap s - and d -wave pairings both in clean and dirty limits (dashed curves). These single-gap curves clearly deviate in the whole temperature range, confirming the multigap nature of superconductivity in Na(Fe_{1-x}Co_x)As (as well as other FeSCs). Surprisingly, $\rho_s(T/T_c)$ of NaFe_{0.95}Co_{0.05}As is virtually the same as that of optimally doped BaP122 ($x = 0.33$, black solid dots), a known nodal isovalent substituted pnictide,²⁰ and shows a notable difference from the exponential saturation in a fully gapped LiFeAs.^{17,18}

Our results show that the superconducting gap even at optimal doping is highly anisotropic in charge-doped Na(Fe_{1-x}Co_x)As. Similar to other FeSCs it becomes more anisotropic upon departure from optimal doping. To explain such sensitivity to the doping level and the appearance of nodes in some materials, several proposals have been put forward: (i) Following a suggestion by Kuroki *et al.* that nodal versus nodeless behavior is controlled by the pnictogen height in the 1111 family,²³ Hashimoto *et al.* extended this suggestion to 111 and 122 families.¹⁸ (ii) The nodal structure of the superconducting gap was linked with the evolution of the Fermi surface topology and orbital content in different bands.^{3,4,26,45,46} The band structure of NaFeAs is significantly different from 122 compounds, which itself varies significantly between different hole, electron, and isovalent substitutions, with no apparent correlation that may explain the appearance of nodes only in some compounds. (iii) Another approach is to incorporate changes in both the band structure and renormalization of intraband and in-band Coulomb interactions. According to Ref. 3: (1) For weak and moderate electron doping, the propensity of s_{\pm} - and d -wave pairing channels are comparable; (2) for weak and moderate hole doping, s_{\pm} pairing is dominant; and (3) for strong electron and hole doping, the d -wave channel is dominant. From this classification, regime (1) seems to be most relevant for optimally doped Na(Fe_{1-x}Co_x)As and

regime (3) is appropriate for the overdoped compositions, consistent with our results.

In conclusion, a combined study of self-doped Na_{1- δ} FeAs and charge-doped Na(Fe_{1-x}Co_x)As establishes the systematics of the superconducting gap evolution with doping in the 111 compounds. Similar to other FeSCs, we find a universal tendency of developing the highest anisotropy at the dome edges. However, we show that, even at optimal doping, the low-temperature penetration depth study indicates a highly anisotropic superconducting gap. In addition, temperature-dependent superfluid density at optimal doping is remarkably similar to $\rho_s(T)$ of isovalent-doped BaFe₂(As_{1-x}P_x)₂, a known nodal pnictide superconductor at optimal doping.

Recently, two studies using crystals from the Xian-Hui Chen group^{37,38} suggested a fully isotropic superconducting gap in NaFe_{1-x}Co_xAs at optimal Co doping. To check if the difference in the conclusions is caused by the difference in the properties of samples of this reactive material, we requested crystals from the Chen group for a cross examination. We received and measured the optimally doped samples with $x = 0.028$. The results were virtually identical (within the noise level) to those presented in Figs. 3 and 4, ruling out the sample dependence of our conclusions. The possible reasons for the discrepancy with other studies are discussed in the Introduction. We also note that superconductivity in Na-deficient NaFeAs may be inhomogeneous and coexist with antiferromagnetic order.

We thank A. Chubukov, P. Hirschfeld, R. Thomale, A. Kaminski, Hai-Hu Wen, X. H. Chen, and Shi-Yan Li for useful discussions. We especially thank X. H. Chen and X. G. Luo for supplying the crystals for a cross-examination study. Work at the Ames Laboratory was supported by the U.S. Department of Energy, Office of Basic Energy Sciences, Division of Materials Sciences and Engineering under Contract No. DE-AC02-07CH11358. The single crystal growth at University of Tennessee was supported by U.S. DOE BES under Grant No. DE-FG02-05ER46202 (P.D.).

*Corresponding author: prozorov@ameslab.gov

¹I. I. Mazin, *Nature (London)* **464**, 183 (2010).

²J. Paglione and R. L. Greene, *Nat. Phys.* **6**, 645 (2010).

³A. Chubukov, *Annu. Rev. Condens. Matter Phys.* **3**, 57 (2012).

⁴P. J. Hirschfeld, M. M. Korshunov, and I. I. Mazin, *Rep. Prog. Phys.* **74**, 124508 (2011).

⁵R. Prozorov and V. G. Kogan, *Rep. Prog. Phys.* **74**, 124505 (2011).

⁶R. T. Gordon, C. Martin, H. Kim, N. Ni, M. A. Tanatar, J. Schmalian, I. I. Mazin, S. L. Bud'ko, P. C. Canfield, and R. Prozorov, *Phys. Rev. B* **79**, 100506 (2009).

⁷C. Martin, H. Kim, R. T. Gordon, N. Ni, V. G. Kogan, S. L. Bud'ko, P. C. Canfield, M. A. Tanatar, and R. Prozorov, *Phys. Rev. B* **81**, 060505 (2010).

⁸M. A. Tanatar, J.-P. Reid, H. Shakeripour, X. G. Luo, N. Doiron-Leyraud, N. Ni, S. L. Bud'ko, P. C. Canfield, R. Prozorov, and L. Taillefer, *Phys. Rev. Lett.* **104**, 067002 (2010).

⁹J.-P. Reid, M. A. Tanatar, X. G. Luo, H. Shakeripour, N. Doiron-Leyraud, N. Ni, S. L. Bud'ko, P. C. Canfield, R. Prozorov, and L. Taillefer, *Phys. Rev. B* **82**, 064501 (2010).

¹⁰C. Ren, Z.-S. Wang, Z.-Y. Wang, H.-Q. Luo, X.-Y. Lu, B. Sheng, C.-H. Li, L. Shan, H. Yang, and H.-H. Wen, [arXiv:1106.2891](https://arxiv.org/abs/1106.2891).

¹¹S. L. Bud'ko, N. Ni, and P. C. Canfield, *Phys. Rev. B* **79**, 220516 (2009).

¹²G. Mu, J. Tang, Y. Tanabe, J. Xu, S. Heguri, and K. Tanigaki, *Phys. Rev. B* **84**, 054505 (2011).

¹³H. Kim, M. A. Tanatar, B. Shen, H.-H. Wen, and R. Prozorov, [arXiv:1105.2265](https://arxiv.org/abs/1105.2265).

¹⁴J.-P. Reid, M. A. Tanatar, X. G. Luo, H. Shakeripour, S. Rene de Cotret, N. Doiron-Leyraud, J. Chang, B. Shen, H.-H. Wen, H. Kim, R. Prozorov, and L. Taillefer, [arXiv:1105.2232](https://arxiv.org/abs/1105.2232).

¹⁵J. K. Dong, S. Y. Zhou, T. Y. Guan, H. Zhang, Y. F. Dai, X. Qiu, X. F. Wang, Y. He, X. H. Chen, and S. Y. Li, *Phys. Rev. Lett.* **104**, 087005 (2010).

¹⁶K. Hashimoto, A. Serafin, S. Tonegawa, R. Katsumata, R. Okazaki, T. Saito, H. Fukazawa, Y. Kohori, K. Kihou, C. H. Lee, A. Iyo, H. Eisaki, H. Ikeda, Y. Matsuda, A. Carrington, and T. Shibauchi, *Phys. Rev. B* **82**, 014526 (2010).

- ¹⁷H. Kim, M. A. Tanatar, Y. J. Song, Y. S. Kwon, and R. Prozorov, *Phys. Rev. B* **83**, 100502 (2011).
- ¹⁸K. Hashimoto, S. Kasahara, R. Katsumata, Y. Mizukami, M. Yamashita, H. Ikeda, T. Terashima, A. Carrington, Y. Matsuda, and T. Shibauchi, *Phys. Rev. Lett.* **108**, 047003 (2012).
- ¹⁹K. Cho, M. A. Tanatar, H. Kim, W. E. Straszheim, N. Ni, R. J. Cava, and R. Prozorov, *Phys. Rev. B* **85**, 020504 (2012).
- ²⁰K. Hashimoto, M. Yamashita, S. Kasahara, Y. Senshu, N. Nakata, S. Tonegawa, K. Ikada, A. Serafin, A. Carrington, T. Terashima, H. Ikeda, T. Shibauchi, and Y. Matsuda, *Phys. Rev. B* **81**, 220501 (2010).
- ²¹M. Yamashita, N. Nakata, Y. Senshu, S. Tonegawa, K. Ikada, K. Hashimoto, H. Sugawara, T. Shibauchi, and Y. Matsuda, *Phys. Rev. B* **80**, 220509 (2009).
- ²²X. Qiu, S. Y. Zhou, H. Zhang, B. Y. Pan, X. C. Hong, Y. F. Dai, M. J. Eom, J. S. Kim, Z. R. Ye, Y. Zhang, D. L. Feng, and S. Y. Li, *Phys. Rev. X* **2**, 011010 (2012).
- ²³K. Kuroki, H. Usui, S. Onari, R. Arita, and H. Aoki, *Phys. Rev. B* **79**, 224511 (2009).
- ²⁴C.-H. Lee, A. Iyo, H. Eisaki, H. Kito, M. T. Fernandez-Diaz, T. Ito, K. Kihou, H. Matsuhata, M. Braden, and K. Yamada, *J. Phys. Soc. Jpn.* **77**, 083704 (2008).
- ²⁵Y. Mizuguchi, Y. Hara, K. Deguchi, S. Tsuda, T. Yamaguchi, K. Takeda, H. Kotegawa, H. Tou, and Y. Takano, *Supercond. Sci. Technol.* **23**, 054013 (2010).
- ²⁶R. Thomale, C. Platt, W. Hanke, J. Hu, and B. A. Bernevig, *Phys. Rev. Lett.* **107**, 117001 (2011).
- ²⁷C. Chu, F. Chen, M. Gooch, A. Guloy, B. Lorenz, B. Lv, K. Sasmal, Z. Tang, J. Tapp, and Y. Xue, *Physica C* **469**, 326 (2009); S. L. Li, C. de la Cruz, Q. Huang, G. F. Chen, T.-L. Xia, J. L. Luo, N. L. Wang, and P. Dai, *Phys. Rev. B* **80**, 020504(R) (2009).
- ²⁸S. J. Zhang, X. C. Wang, Q. Q. Liu, Y. X. Lv, X. H. Yu, Z. J. Lin, Y. S. Zhao, L. Wang, Y. Ding, H. K. Mao, and C. Q. Jin, *Europhys. Lett.* **88**, 47008 (2009).
- ²⁹M. Gooch, B. Lv, J. H. Tapp, Z. Tang, B. Lorenz, A. M. Guloy, and P. C. W. Chu, *Europhys. Lett.* **85**, 27005 (2009).
- ³⁰K. Kitagawa, Y. Mezaki, K. Matsubayashi, Y. Uwatoko, and M. Takigawa, *J. Phys. Soc. Jpn.* **80**, 033705 (2011).
- ³¹D. R. Parker, M. J. P. Smith, T. Lancaster, A. J. Steele, I. Franke, P. J. Baker, F. L. Pratt, M. J. Pitcher, S. J. Blundell, and S. J. Clarke, *Phys. Rev. Lett.* **104**, 057007 (2010).
- ³²G. F. Chen, W. Z. Hu, J. L. Luo, and N. L. Wang, *Phys. Rev. Lett.* **102**, 227004 (2009).
- ³³D. R. Parker, M. J. Pitcher, P. J. Baker, I. Franke, T. Lancaster, S. J. Blundell, and S. J. Clarke, *Chem. Commun.* **2009**, 2189.
- ³⁴Z.-H. Liu, P. Richard, K. Nakayama, G.-F. Chen, S. Dong, J.-B. He, D.-M. Wang, T.-L. Xia, K. Umezawa, T. Kawahara, S. Souma, T. Sato, T. Takahashi, T. Qian, Y. Huang, N. Xu, Y. Shi, H. Ding, and S.-C. Wang, *Phys. Rev. B* **84**, 064519 (2011).
- ³⁵S. V. Borisenko, V. B. Zabolotnyy, D. V. Evtushinsky, T. K. Kim, I. V. Morozov, A. N. Yaresko, A. A. Kordyuk, G. Behr, A. Vasiliev, R. Follath, and B. Büchner, *Phys. Rev. Lett.* **105**, 067002 (2010).
- ³⁶N. Qureshi, P. Steffens, Y. Drees, A. C. Komarek, D. Lamago, Y. Sidis, L. Harnagea, H.-J. Grafe, S. Wurmehl, B. Büchner, and M. Braden, *Phys. Rev. Lett.* **108**, 117001 (2012).
- ³⁷H. Yang, Z. Wang, D. Fang, T. Kariyado, G. Chen, M. Ogata, T. Das, A. V. Balatsky, and H.-H. Wen, *arXiv:1203.3123*.
- ³⁸A. F. Wang, X. G. Luo, Y. J. Yan, J. J. Ying, Z. J. Xiang, G. J. Ye, P. Cheng, Z. Y. Li, W. J. Hu and X. H. Chen, *Phys. Rev. B* **85**, 224521 (2012).
- ³⁹C. He, Y. Zhang, B. P. Xie, X. F. Wang, L. X. Yang, B. Zhou, F. Chen, M. Arita, K. Shimada, H. Namatame, M. Taniguchi, X. H. Chen, J. P. Hu, and D. L. Feng, *Phys. Rev. Lett.* **105**, 117002 (2010).
- ⁴⁰I. Todorov, D. Y. Chung, H. Claus, C. D. Malliakas, A. P. Douvalis, T. Bakas, J. He, V. P. Dravid, and M. G. Kanatzidis, *Chem. Mater.* **22**, 3916 (2010).
- ⁴¹M. A. Tanatar, N. Spyrisson, K. Cho, E. C. Blomberg, G. Tan, P. Dai, C. Zhang, and R. Prozorov, *Phys. Rev. B* **85**, 014510 (2012).
- ⁴²R. Prozorov, R. W. Giannetta, A. Carrington, and F. M. Araujo-Moreira, *Phys. Rev. B* **62**, 115 (2000).
- ⁴³R. Prozorov and R. W. Giannetta, *Supercond. Sci. Technol.* **19**, R41 (2006).
- ⁴⁴V. G. Kogan, C. Martin, and R. Prozorov, *Phys. Rev. B* **80**, 014507 (2009).
- ⁴⁵R. Thomale, C. Platt, W. Hanke, and B. A. Bernevig, *Phys. Rev. Lett.* **106**, 187003 (2011).
- ⁴⁶A. Nicholson, W. Ge, X. Zhang, J. Riera, M. Daghofer, A. M. Oleś, G. B. Martins, A. Moreo, and E. Dagotto, *Phys. Rev. Lett.* **106**, 217002 (2011).